Superelastic percolation network of polyacrylamide (PAAm)–kappa carrageenan (κC) composite

G. Akin Evingür · Ö. Pekcan

Abstract The elasticity of the polyacrylamide (PAAm)-kappa carrageenan (κC) composite was determined as a function of (w/v-%) κC content at 40 °C. The gel composites studied contained various percentages (w/v-%) of κC. The elasticity of the swollen PAAm-κC composite was characterized by using the tensile testing technique. This study investigated the elasticity and the percolation threshold of PAAm-κC composite as a function of κC content. It is understood that the compressive elastic modulus decreases up to 1 (w/v-%) of κC and then increases at contents above 1(w/v-%) of κC. The critical exponent of elasticity y was determined between 1 and 1.6 (w/v-%) of κC and found to be 0.68. The observed elastic percolation threshold is consistent with the suggested values of the *superelastic percolation network*.

Keywords Universality · Elasticity · Acrylamide · Kappa carrageenan (κC) · Superelastic percolation network

G. A. Evingür
Piri Reis University, 34940 Tuzla, Istanbul, Turkey

Ö. Pekcan (✉)
Kadir Has University, 34083 Cibali, Istanbul, Turkey
e-mail: pekcan@khas.edu.tr

Introduction

Composites can be defined as a substance composed of two or more materials with different base structures combined in such a way that the end product has different properties than either of the parent materials (Friedrich et al. 2005). Polyacrylamide (PAAm) can be polymerized easily by free radical crosslinking copolymerization (FCC) of acrylamide (AAm) in the presence of N,N'-methylenebisacrylamide (MBA) as the crosslinker. Biological hydrogels, e.g., κ carrageenan (κC) is a gel type that has the high ability of biological gels to absorb different substances. The low and high water sorption properties of hydrogels are important for the use of sorbents of biomaterials and separation operations in biotechnology, drug delivery systems, processing of agricultural products and sensors. In our previous studies, the steady-state fluorescence (SSF) technique was employed to investigate the gelation (Aktaş et al. 2006) and swelling of PAAm-κC gels at various temperatures (Evingür and Pekcan 2012a).

Since the various microscopic elasticity models have predicted different critical exponents, the static elasticity of random percolating structures is of particular interest. Percolation systems, being fractal, manifest similar behaviors (Schriemer et al. 1996). The first experimental system in which these predictions were tested consisted of sintered metal powders. The relation between percolation theory and the elasticity of gels was discovered theoretically (de Gennes

1976). The macroscopic conductance of a resistor network with a fraction p of conducting links and the elastic modulus E of a gel was obtained by polymerization of z-functional units. Bond percolation on elastic networks involving nearest neighbor forces was studied by numerical simulations (Feng and Sen 1984). With purely central forces, the bulk and shear module go to zero, with exponent f and at a threshold p_{cen}. The elastic properties of random percolating systems in the critical region were studied (Kantor and Webman 1984). The Hamiltonian was chosen to correctly represent the elastic behavior of continuous random composites made up of rigid and soft regions near the percolation threshold. This result is relevant to experiments on such systems. The critical exponent and transitions in swollen polymer networks and in linear macromolecules were performed (Erman and Flory 1986). Critical behavior was found for the single and long chain limit. Bond and site percolations on two- and three-dimensional elastic and superelastic percolation networks with central forces were studied using large-scale Monte Carlo simulations and finite size scaling analysis (Arbabi and Sahimi 1993). The critical exponents of the elastic modulus and correlation length of the system for the *bcc* network were found. The elastic modulus and equilibrium swelling of near critical gels were performed theoretically (Rubinstein and Colby 1994). The concentration dependence of the modulus when the gel was diluted in a good solvent was also calculated and used to predict the maximum swelling. The mechanical properties of κ-carrageenan in a high concentration of sugar solutions were also studied (Loret et al. 2009), which gave new insights into the molecular state of carrageenan in the presence of high concentrations of sugars. Compressive elastic modulus of polyacrylamide hydrogels and semi-IPN's with poly(*N*-isopropylacrylamide) (PNIPAAm) was performed (Muniz and Geuskens 2001). Semi-IPN hydrogels presented better mechanical properties than PAAm hydrogel, mainly when the PNIPAAm chains are in a collapsed state. A superabsorbent hydrogel composite made of cellulose nanofibrils and chitosan-graft-polyacrylic acid was developed (Spagnol et al. 2012a). The composite was analyzed by FTIR, XRD and SEM. Superabsorbent hydrogel nanocomposites based on a starch-g-poly (sodium acrylate) matrix filled with cellulose nanowhiskers (CNWs) were evaluated (Spagnol et al. 2012b). The swelling kinetics and mechanical properties of CNWs were improved. In addition, we studied the elastic percolation of a swollen PAAm-multiwall carbon nanotube (MWNTs) composite, which shows that the compressive elastic modulus increases dramatically up to 1 (wt) % MWNT by increasing the nanotube content and then decreases, presenting a critical MWNT value indicating that there is a sudden change in the material elasticity (Evingür and Pekcan 2012a). The critical exponent, y, of elasticity below the critical MWNT content 1 (wt) % is found to be 0.58, which is consistent with the suggestions of percolation in the *superelastic percolation network* (SEPN) for the PAAm-MWNT composite.

The aim of the present study is to understand the effect of κC content on the elastic behavior of swollen PAAm-κC composites and experimentally determine the critical exponent of elasticity. In this study, it was observed that the elastic properties of PAAm-κC composites are highly dependent on κC content, which directly influences monomer interactions between PAAm and κC in the composites. Such monomer interactions will play a critical role in load transfer and interfacial bonding, which determine the elastic properties of the composites. Elastic percolation occurs at 1.0 (w/v-%) of κC with a critical exponent of around $y \approx 0.68$, which is close to the theoretical prediction of this value in the 3D percolated system known as a SEPN. The elastic percolation threshold agrees with the suggestions of percolation for SEPN and the critical theory for PAAm-κC composites.

Experiment

Preparation of PAAm-κC composite

Polyacrylamide (PAAm)-kappa carrageenan (κC) composites were formed by FCC as follows: 0.71 g of AAm (acrylamide, Merck), 0.01 g of MBA (*N*,*N'*-methylenebisacrylamide, Merck), 0.008 g of APS (ammonium persulfate, Merck) and 2 μl of TEMED (tetramethylethylenediamine, Merck) were dissolved in 5 ml distilled water by heating. The heated mixture solution was held at 80 °C. Then varying percentages (w/v-%) of κC were added for the preparation of the composite gels. The solution was stirred (200 rpm) for 15 min to achieve a homogeneous solution. All samples were deoxygenated by bubbling nitrogen for

10 min just before the polymerization process (Aktaş et al. 2006). The gelation (Aktaş et al. 2006), drying (Evingür and Pekcan 2011) and swelling (Evingür and Pekcan 2012b) processes were performed by a Model LS-50 spectrometer from PerkinElmer, equipped with a temperature controller.

Compressive elastic measurements

After gelation (Aktaş et al. 2006), the composites prepared with various percentages (w/v-%) of κC contents were cut into disks with a 10-mm diameter and 4-mm thickness. Three samples were also prepared from κC contents, and all experiments were repeated three times. Before the compression measurements, the composites were maintained in distilled water at 40 °C to achieve swelling equilibrium. A final wash of all samples with distilled water was carried out for 1 week at a desired temperature to remove unreacted monomers and to allow the gel to achieve swelling equilibrium. The mechanical experiments of PAAm-κC composites were performed at 40 °C. A Hounsfield H5 K-S model tensile testing machine, set at a crosshead speed of 1.0 cm/min, probe size of 2 cm and load cell of 5 N sensibility, was used to perform uniaxial compression experiments on the samples of each type of composite. Figure 1 shows the behaviors of the PAAm-κC composites before and after applying the uniaxial compression. Figure 1a corresponds to the initial state, i.e., zero loads, and Fig. 1b presents the gel under 5 N, respectively. Loss of water and changes in temperature during the measurements were not observed because the compression period was less than 1 min. Just before starting the experiment, we made a correction indicating that the curve in Fig. 2 is smaller at low deformations because of the nominal surface. All samples presented this behavior. The experimental data in all compression experiments that obtained up to about 5 % of deformation were rejected as given in Muniz and Geuskens (2001).

There was no deswelling during the compressive deformation stage, which means that our experiment corresponds to the case in which we can assume a uniform compressive elastic modulus S, which for each composite was determined from the slope of the linear portions of compression stress-strain curves using the equation of state for rubber elasticity. The statistical thermodynamics equation of state for rubber elasticity is indicated below:
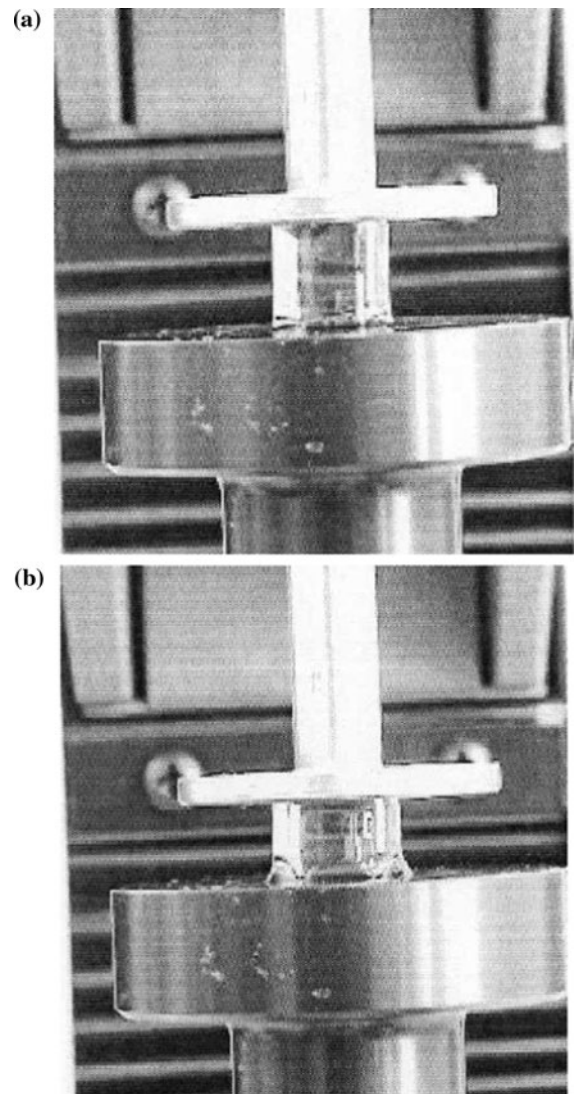

Fig. 1 Compression process of 0.5 (w/v-%) of κC **a** initial ($F = 0.0$ N) and **b** final states ($F = 5.0$ N)
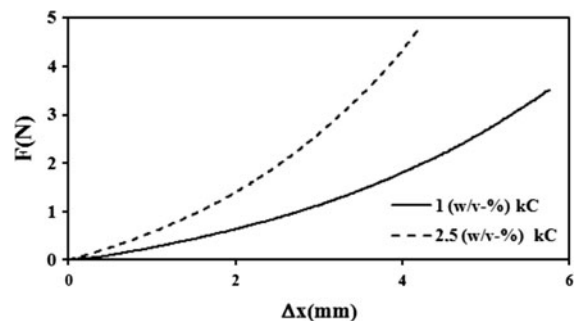

Fig. 2 The force F(N) and compression (mm) curves for 1 and 2.5 (w/v-%) of κC content at 40 °C, respectively

$$\tau = \left(\frac{\partial A}{\partial \lambda}\right)_{T,V} = \frac{\rho RT}{\overline{M_c}} \frac{\overline{r_0^2}}{r_f^2} \lambda \qquad (1)$$

Here, τ is the shear stress per unit area, ρ is the density of the polymer, $\overline{M_c}$ is the number-average molecular weight between crosslinks, and λ is the extension/compression ratio. The extension/compression ratio λ changes according to different theories (Nielsen and Lawrence 1994). The quantity $\frac{\overline{r_0^2}}{r_f^2}$ is the front factor and is the ratio of the end-to-end distance in a real network versus the end-to-end distance of isolated chains. Equation 1 assumes that the network is ideal in that all chains are elastically active and contribute to the elastic stress. From the constitutive relationship, the shear modulus S is then

$$S = \frac{\rho RT}{\overline{M_c}} \frac{\overline{r_0^2}}{r_f^2} \left(1 - \frac{2\overline{M_c}}{\overline{M_n}}\right) \qquad (2)$$

and the force per unit area is

$$\tau = S\lambda \qquad (3)$$

where $\lambda = \frac{\Delta l}{l_0}$, $\Delta l = l - l_0$, l is the last distance and l_0 the initial distance. Note the dependence of the shear modulus on $\overline{M_c}$. Also, the stress-strain behavior of rubbery elastic materials is nonlinear. The equations are less applicable and invalid at higher elongations ($\lambda > 3$) (Anseth et al. 1996). On the other hand, toughness is determined by the underside area of linear portions of compression stress-strain curves.

Results and discussion

Forces (F) or loads corresponding to compression (mm) were obtained from the original curves of uniaxial compression experiments. The force F(N) versus compression (mm) curves of 1 and 2.5 (w/v-%) of κC at 40 °C are shown in Fig. 2. The repulsive force between monomers increases rapidly when the bond length is shortened from the equilibrium position. When the κC content in the composite is increased, then the repulsive force is increased as seen in Fig. 2. The reason for this can be explained thermodynamically in that a decrease in length brings about an increase in entropy because of changes in the end-to-end distances of the network chains in PAAm-κC composite gels.

Stress (Pa)-strain plots for the composites were drawn by using the data obtained from the linear region observed in the plots of F(N) versus compression curves for 0, 1 and 2.5 (w/v-%) of κC content gels at 40 °C in Fig. 3. The stress-strain curves display a good linear relationship at 40 °C, which agrees with Eq. 3. The compressive elastic modulus was obtained by a least square fit to the linear region observed. The produced values of the compressive elastic modulus versus κC are listed in Table 1. For pure PAAm gels, the value of the compressive elastic modulus is 0.0410 MPa at 40 °C. The compressive elastic modulus presents a maximum value for pure acrylamide (0 (w/v-%) of κC). The addition of κC first increased and then decreased the modulus of the composite below and above 1 (w/v-%) of κC, respectively. The composite has a smaller initial stress-strain slope for 1 (w/v-%) of κC than 2.5 (w/v-%) of κC. In this case, it appears that the increasing entropy resulting from the decrease in length plays an important role for obtaining the varying onset behavior. The stress of the PAAm-κC composite increases dramatically when the strain exceeds about 0.45 % strain for 2.5 (w/v-%) of κC where the κC monomers take responsibility in the composite. In Fig. 3, the increase in the slope of the stress-strain curve for higher κC content can be explained by the increase of κC, which forms a superelastic network that significantly improves the stress relaxation of the composite. As the composite gel became more swollen, rapid water absorbency was achieved at 40 °C. The swelling capacity of the composites was recognized to be affected by alkaline

Table 1 Some experimental and calculated parameters of PAAm-κC composites

PAAm	κC (w/v-%)	S (MPa)
2 M	0	0.041
	0.5	0.051
	0.6	0.018
	0.8	0.016
	1.0	*0.009*
	1.2	0.009
	1.4	0.018
	1.5	0.026
	2.0	*0.039*
	2.5	0.041
	3	0.041

hydrolysis, and osmotic pressure, in turn, results in a carboxylate anion increment and consequently absorbency enhancement. The decrease in the swelling capacity may be attributed to alkaline degradation of the κC part of the hydrogel over 40 °C. Therefore, the composites behave exothermically between 30 and 40 °C and endothermically between 40 and 60 °C during swelling processes (Evingür and Pekcan 2012b).

Figure 4 shows the variation of the compressive elastic modulus versus the content of κC in the composite, which can be divided into three regions such as the (1) *inductive region*, which explains the decrease in elasticity for the low level of κC loading, (2) *percolation region*, which explains the increase in double helices due to the formation of continuous elastic networks in the composite, and (3) *saturation region*, which represents the upper part of the elasticity, indicating the marginal effect of double helices due to further addition of κC in the composite (Çakir and Foegeding 2011). The sudden increase in S predicts that the composite has reached a super-elastic percolation network in the percolation region. In order to decide the location of the percolation threshold, the derivative of the compressive elastic modulus with respect to (w/v-%) of the κC content was taken using the Matlab program of moving derivatives. The percolation threshold was found to be 1.0 (w/v-%) of κC where the composite attained elastic and super-elastic equilibrium, exhibiting a high degree of PAAm and κC monomer interactions and/or entanglement. The effect of increasing κC content in reducing the swelling and increasing compressive elastic modulus was an expected result for composite behavior in the percolation region. This can be explained by a decrease in length bringing about an increase in
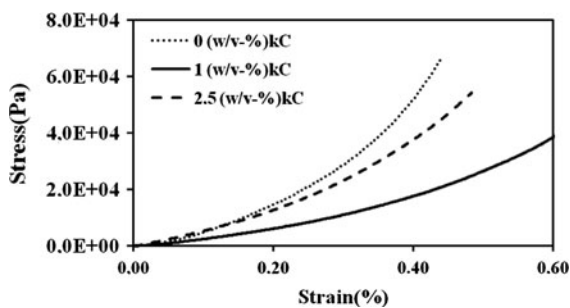
Table 2 Critical exponents for elastic and superelastic percolation networks for three dimensions and in the mean field approximation (Sahimi 1994)

	x	y
$d = 3$	2.1	0.65
$d \geq 6$	3	0

entropy because of changes in the end-to-end distances of the network chains of PAAm-κC composites. Thus, the entropic model for composite elasticity is a reasonable approximation. In other words, the effect of increasing κC content in increasing the compressive elastic modulus is an expected result in the percolation region. The increase in the compressive elastic modulus can be explained in that the collapsed phase has a network structure with double helices just like the swollen phase. On the other hand, the compressive elastic modulus increases because it is known that the swelling and hence the osmotic (bulk) modulus decreases as κC is added to the composite. The compressive elastic modulus increases as κC is added because the free chain size decreases (Çakir and Foegeding 2011).

Lastly, we believe in that the elastic properties of PAAm-κC composites are highly dependent on κC content, which directly influences PAAm-κC monomers' interactions in the composites. Such monomer interactions will play a critical role in the load transfer and interfacial bonding that determines the elastic properties of the composites. The variations in the κC content in the resultant composites could be the major reason for this phenomenon.
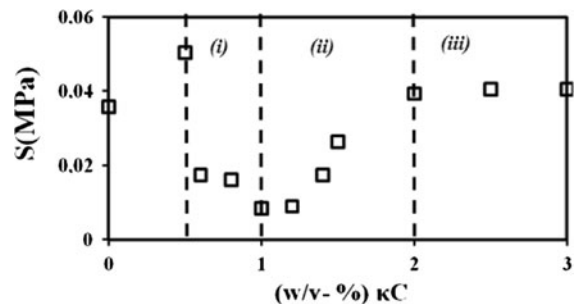

Fig. 3 Stress-strain curves for 0, 1 and 2.5 (w/v-%) of κC content at 40 °C

Fig. 4 Dependence of the compressive elastic modulus on the concentration of (w/v-%) of κC in the composite at 40 °C. (*i*), (*ii*) and (*iii*) show the *inductive*, *percolation* and *saturation region*, respectively

Consider a percolation network whose bonds represent elastic springs that can be stretched and/or bent (Sahimi 1994). As a model of disordered materials, each bond on the disordered materials represents an elastic element, or a spring, with an elastic constant e, and the rest have an elastic constant b, which can take on values from a probability density function $H(e)$. In most cases, the binary distribution

$$H(e) = p\delta(e - a) + (1 - p)\delta(e - b) \quad (4)$$

e takes the values a and b with probability p and $1 - p$, respectively. If $b = 0$ and a is finite, the system is called an *elastic percolation network* (EPN) and defines S_e as the effective elastic module of the network. If $a = \infty$ and b is finite, a fraction p of the springs is totally rigid and the rest are soft, the system is called a SEPN and defines S_s as the effective elastic module of a superelastic percolation network. As the percolation threshold p_c of an EPN is approached from above, all of the compressive elastic modulus S of the system vanishes. Near the percolation threshold, p_c, the effective elastic module of the network S_e obeys the following scaling law (Sahimi 1994)

$$S_e(p) \approx (p - p_c)^x \quad (5)$$

where x is the critical exponent for EPN. In contrast, in an SEPN all compressive elastic moduli diverge as p_c is approached from below according to

$$S_s(p) \approx (p_c - p)^{-y} \quad (6)$$

where y is the critical exponent for SEPN. x and y are given in Table 2, which includes the critical exponents of elastic and superelastic percolation networks for three dimensions and in the mean field approximation (Sahimi 1994). Using this scaling description for S_e and S_s, the upper and lower bounds for the exponent can be found

$$\Delta = \frac{x}{x + y} \quad (7)$$

If $x = 1.9 - 2.1$ can be used for the chemical gels and Eq. (6) can be used for estimating y, the following is obtained

$$0.61 \leq \Delta \leq 0.75 \quad (8)$$

where the lower and upper limits correspond to the Rouse and Zimm regimes, respectively.

The value of the fitting exponent y in Eq. 6 was estimated from the slope of the linear relation between log S and log $Ip-p_cI$ at $p < p_c$ as shown in Fig. 5. Below 1 (w/v-%) of κC, nonuniversal behavior might be explained by the samples corresponding to different areas of the static crossover between the mean field and the critical percolation (Colby et al. 1993). The elastic percolation threshold occurs at 1.0 (w/v-%) of κC in the percolation region (as shown in Fig. 4) with a critical exponent around $y \approx 0.68$, which is close to the theoretical prediction of this value in the 3D percolated system known as a SEPN. The critical exponent y agrees with the literature (see Table 2) (Colby et al. 1993; Sahimi 1994). x is the critical exponent, which is taken from the literature with the limit $x = 1.9–2.1$. Moreover, Δ was found to be very close to the upper limit of Δ as given in Eq. 8. If the universality of any system is known, it provides universal laws that determine the geometrical and physical properties of the system (Berkowitz and Balberg 1993).

Conclusions

The compressive elastic modulus' measurement of PAAm-κC composites was characterized with a tensile testing machine. The behavior of the compressive elastic modulus was explained in the following way: a decrease in length brings about an increase in entropy because of changes in the end-to-end distances of the network chains of PAAm-κC composites thermodynamically. Thus, the entropic model for composite elasticity is a reasonable approximation. Elastic percolation occurs between 1.0 and 1.6 (w/v-%) of κC with the critical exponent of $y = 0.68$, which is
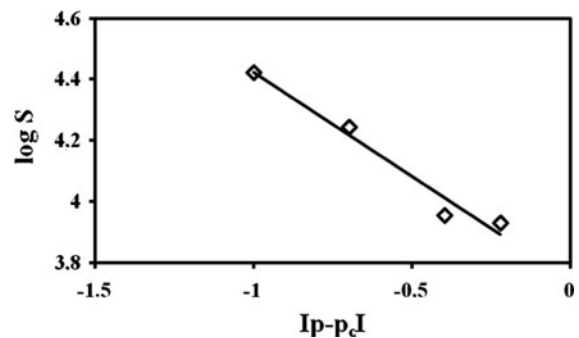
Fig. 5 Logarithmic plot of the compressive elastic modulus versus (w/v-%) of contents curves for $p < p_c$. The y exponent ($y = 0.68$) was determined from the slope of the straight line

close to the theoretical prediction of this value in a 3D percolated system ($y = 0.65$) (Colby et al. 1993; Sahimi 1994). The percolation critical exponent y obtained from fitting the composition dependence of the compressive elastic modulus below (1.6 (w/v-%) of κC) is consistent with the suggestions of percolation for SEPN (see Table 2) and the 3D percolated system for PAAm-κC composites.

References

Aktaş DK, Evingür GA, Pekcan Ö (2006) Universal behaviour of gel formation from acrylamide-carrageenan mixture around the gel point: a fluorescence study. J Biomol Struct Dyn 24(1):83–90

Anseth KS, Bowman CN, Peppas LB (1996) Mechanical properties of hydrogels and their experimental determination. Biomaterials 17:1647–1657

Arbabi S, Sahimi M (1993) Mechanics of disordered solids. I. percolation on elastic networks with central forces. Phys Rev B 47(2):695–702

Berkowitz B, Balberg I (1993) Percolation theory and its application to groundwater hydrology. Water Res 29(4): 775–794

Çakır E, Foegeding EA (2011) Combining protein micro protein micro phase separation and protein-polysaccharide segregative phase separation to produce gel structures. Food Hydrocoll 25:1538–1546

Colby RH, Gillmor JR, Rubinstein M (1993) Dynamics of near critical polymer gels. Phys Rev E 48(5):3712–3716

de Gennes PG (1976) On the relation between percolation theory and the elasticity of gels. Le J de Phys Lett 37:L1–L2

Erman B, Flory PJ (1986) Critical phenomena and transitions in swollen polymer networks and in linear macromolecules. Macromol 19:2342–2353

Evingür GA, Pekcan Ö (2011) Drying of polyacrylamide composite gels formed with various kappa carrageenan content. J Fluo 21:1531–1537

Evingür GA, Pekcan Ö (2012a) Elastic percolation of swollen polyacrylamide (PAAm)-multiwall carbon nanotubes (MWNTs) composite. Ph Transitions 85:553–564

Evingür GA, Pekcan Ö (2012b) Temperature effect on the swelling of PAAm–kcarrageenan composites. J Appl Polym Sci 123:1746–1754

Feng S, Sen PN (1984) Percolation on elastic networks: new exponent and threshold. Phys Rev Lett 52(3):216–219

Friedrich K, Fakirov S, Zhang Z (2005) Polymer composites from nano to macro scale. Springer, USA

Kantor Y, Webman I (1984) Elastic properties of random percolating systems. Phys Rev Lett 52(21):1891–1894

Loret C, Ribelles P, Lundin L (2009) Mechanical properties of k-carrageenan in high concentration of sugar solutions. Food Hydrocoll 23:823–832

Muniz EC, Geuskens G (2001) Compressive elastic modulus of polyacrylamide hydrogels and semi-IPN's with poly (N-isoproplacrylamide). Macromolecules 34:4480–4484

Nielsen LE, Lawrence RF (1994) Mechanical properties of polymers and composites. Marcel Dekker, New York

Rubinstein RH, Colby H (1994) Elastic modulus and equilibrium swelling of near critical gels. Macromolecules 27: 3184–3190

Sahimi M (1994) Application of percolation theory. Taylor and Francis, London

Schriemer HP, Pachet NG, Page JH (1996) Ultrasonic investigation of the vibrational modes of a sintered glass-bead percolation system. Waves Random Media 6:361–386

Spagnol C, Rodrigues FHA, Pereira AGB, Fajardo AR, Rubira AF, Muniz EC (2012a) Superabsorbent hydrogel composite made of cellulose nanofibrils and chitosan-*graft*-poly (acrylic acid). Carbohydr Polym 87(3):2038–2045

Spagnol C, Rodrigues FHA, Pereira AGB, Fajardo AR, Rubira AF, Muniz EC (2012b) Superabsorbent hydrogel nanocomposites based on starch-g-poly(sodium acrylate) matrix filled with cellulose nanowhiskers. Cellulose 19(4): 1225–1237